Nano Energy (2016) 19, 471–475

Available online at www.sciencedirect.com

ScienceDirect

journal homepage: www.elsevier.com/locate/nanoenergy

RAPID COMMUNICATION

Broadband light absorption enhancement in ultrathin film crystalline silicon solar cells with high index of refraction nanosphere arrays

Baomin Wang[a], Tongchuan Gao[a], Paul W Leu[a,b,*]

[a]Department of Industrial Engineering, University of Pittsburgh, Pittsburgh, PA 15261, United States
[b]Department of Mechanical Engineering and Materials Science, University of Pittsburgh, Pittsburgh, PA 15261, United States

Received 20 August 2015; accepted 30 October 2015
Available online 10 November 2015

KEYWORDS
C-silicon;
Photovoltaics;
Dielectric nanospheres;
Light trapping

Abstract
In this paper, we demonstrate that dielectric nanosphere arrays can enhance the absorption in ultrathin film crystalline silicon by coupling incident light to the underlying silicon layer. By introducing dielectric nanospheres on top of the crystalline silicon thin film solar cell, the power conversion efficiency can be improved by 26.5%. The nanosphere coating increases the absorption and external quantum efficiency over a broadband wavelength range.

Introduction

Ultrathin film crystalline silicon (c-Si) photovoltaics have advantages over conventional bulk c-Si solar cells such as less material usage and lower cost. Not only do thin films use less material, but they enable the use of poorer quality material with shorter minority carrier diffusion lengths since carriers do not have to diffuse as far to be collected. Flexible solar cells may also be enabled when the c-Si is under about 60 μm thick [1–3]. However, the main challenge with c-Si is it is not a strong absorber of sunlight in the near-infrared region. Si is an indirect band gap material and thus photons with energy just above the band gap require phonon interactions for absorption. Different light trapping strategies are thus important for increasing the photon optical length, the distance a photon travels in the c-Si before escaping, in order to increase absorption.

Recently, we demonstrated through simulations that high index of refraction dielectric nanospheres (NSs) on the frontside of c-Si thin film structures can improve efficiencies substantially by coupling incident light into the underlying

*Corresponding author.
E-mail address: pleu@pitt.edu (P. W Leu).
URL: http://www.pitt.edu/~pleu/Research/ (P. W Leu).

http://dx.doi.org/10.1016/j.nanoen.2015.10.039
2211-2855/

absorber layer [4]. This approach of light trapping differs from other approaches such as structuring the active material or using metal nanostructures in that no new surfaces or interfaces are created. Various nanostructures such as nanowires [5-9], nanoholes [10,8], or nanocones [11-13] and metal nanostructures such as nanoparticle arrays [14,15] and nanogrooves [16] have been studied. In these other approaches, additional surfaces or Si/metal interfaces result in higher internal losses from increased surface recombination. Dielectric nanosphere arrays may be scalably coated onto large area solar cells with a variety of nanosphere lithography approaches [17-19] and could offer benefits to cost reduction in photovoltaics. Lin et al. recently reported that dielectric nanosphere monolayers can act as an antireflection layer to increase efficiencies from 5.1% to 6.2% in bulk c-Si solar cells [20]. These conventional bulk solar cells are typically several hundred microns thick and rigid.

In this work, we demonstrate significant efficiency and external quantum efficiency (EQE) enhancement on ultrathin c-Si solar cells of 15 μm thickness via nanosphere coatings. Ultrathin c-Si solar cells exhibit a power conversion efficiency (PCE) of 4.9%. By coating these solar cells with a monolayer of polystyrene (PS) NSs, the PCE increases to 6.2%, which represents a 26.5% power conversion efficiency improvement. The EQE is enhanced by almost two times at some wavelengths. The PS nanospheres allow light to better to couple into the underlying c-Si and thus increase absorption and EQE across a broad range of wavelengths.

Results and discussion

Fig. 1(a) shows a schematic of our ultrathin film c-Si solar cell structure which consists of a c-Si film between an indium tin oxide (ITO) front transparent electrode and a Ti/Ag back contact. The c-Si layer is doped n+, p, and p+ from top to bottom. In order to demonstrate the advantages of nanosphere arrays, a close packed hexagonal lattice monolayer of polystyrene (PS) NSs is coated on top of the c-Si thin film solar cell. Fig. 1(b) shows a scanning electron microscope (SEM) image of the top view of the PS NS hexagonal array. The NS layer is close packed and uniform over the solar cell. Fig. 1(c) shows a cross section SEM image of the solar cell. The c-Si film is about 15 μm thick and the ITO thin film is about 200 nm thick. The ITO has about 85% transparency with sheet resistance $R_s \approx 30-40\ \Omega/\text{sq}$. We used 800 nm diameter PS NSs on top of the ultrathin Si solar cell, because our simulation results (see Supplementary Information) indicate that the ultimate efficiency is relatively insensitive to PS NS diameters above 700 nm. Larger diameter NSs are difficult to coat uniformly on substrates and may also exhibit higher parasitic absorption from impurities.

The ultrathin c-Si film was fabricated from double-side polished p-type (100) Si wafers (100 mm diameter, $10-20\ \Omega$ cm, $475-525$ μm thickness). The wafer was immersed in 25% KOH solution at 90 °C for about 2.5 h to obtain about 15 μm thick Si films [3]. The free standing ultrathin Si film was mounted onto a bulk Si wafer via heat release tape. To dope the substrate n+, phosphorus spin-on dopant (SOD) (P8545, Honeywell Accuspin) was spin coated onto the wafer at 4000 rpm for 1 min and then baked for 1 min at 150 °C. Then the Si film was released, flipped over and mounted on another bulk Si wafer. Boron SOD (B40, Honeywell Accuspin) was spin coated at 4000 rpm for 1 min and then baked for 1 min at 150 °C. The dopants were diffused into the ultrathin Si film by rapid thermal annealing at 900 °C for 15 min. After doping, the Si film was immersed in 7:1 BOE solution for 3 min to remove SOD residue on both sides of the film, and then washed with deionized water

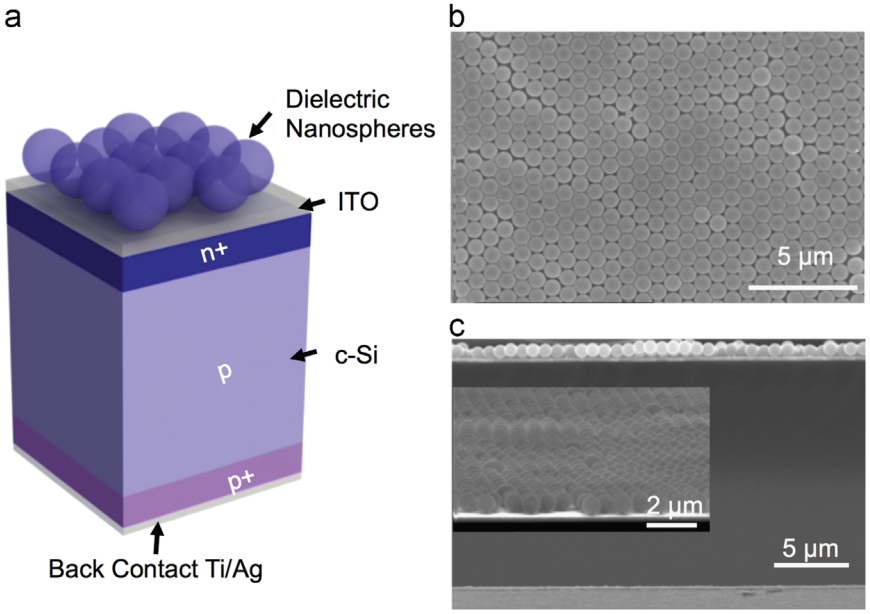

Fig. 1 (a) Schematic of the dielectric nanosphere solar cell. The ultrathin film crystalline silicon (c-Si) has ITO as the front contact and Ti/Ag as the back contact. A hexagonal close packed-monolayer of PS NSs lies on top of this solar cell. (b) Top view SEM image of the PS NSs on Si solar cell. (c) Cross section view of the solar cell with PS NSs monolayer on top. The inset shows a high magnification view of of the NSs at 80°.

thoroughly. 200 nm of ITO was deposited on the n+ side of the Si film via radio frequency (RF) sputtering at 50 W power and 16 mTorr pressure condition. Then 8 nm of Ti followed by 200 nm of Ag was evaporated on the back side of the Si film as back contact. For the PS monolayer fabrication, 4 wt% aqueous suspension (Life Technologies) of 800 nm diameter PS NSs was diluted with equal volume of anhydrous ethanol. A close-packed PS monolayer was fabricated on a water surface via self assembly method [17], transferred on top of the Si film solar cell, and then dried in air.

Fig. 2 plots the current density versus voltage (*J*-*V*) curves of the solar cells measured under the illumination of an AM1.5 global solar simulator. The solar cell without the nanospheres (plain Si) has a short circuit current density J_{sc} of 16.2 mA/cm^2. After coating with PS NSs, the J_{sc} increased to 18.6 mA/cm^2. The short circuit current density increases by about 15%, which indicates an enhancement of incident light absorption in the Si film layer. Table 1 lists the J_{sc}, open circuit voltage (V_{oc}), fill factor (*FF*), and PCE of the solar cells consisting of plain c-Si and with PS NSs on top.

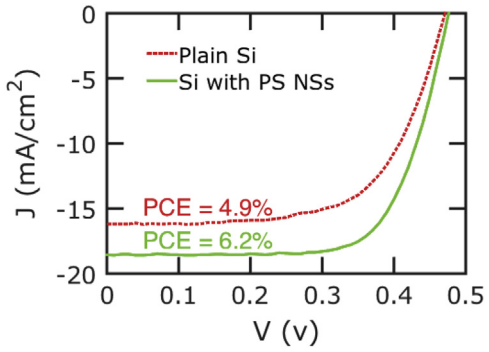

Fig. 2 *J*-*V* characteristics measured on c-Si solar cells without and with PS NSs coating.

Table 1 Photovoltaic properties of the ultrathin c-Si solar cells without and with PS NSs.

Solar Cell Type	J_{sc} (mA/cm^2)	V_{oc} (v)	FF (%)	PCE (%)
Plain Si	16.2	0.47	64	4.9
With PS NSs	18.6	0.48	70	6.2

Along with the increase in J_{sc}, the V_{oc} and *FF* both improve slightly as well. As a result, the PCE of Si solar cell with PS NSs coating increased from 4.9% for the plain Si film solar cell to 6.2%. This is an improvement of about 26.5%.

Based on our experiments, we found the best efficiency enhancements with nanospheres made of PS, which has an index of refraction of about 1.6 [21]. In our previous simulation paper, we found that higher index of refraction NSs exhibits better efficiency improvements [4]. Higher index of refraction NSs has an increased number of whispering gallery modes that can couple incident light to Fabry-Pérot-like resonances and higher order photonic waveguide modes in the Si thin film. However, TiO_2, which has an index of refraction of about 3 [22], also exhibits parasitic absorption in the ultraviolet [23]. Current synthesis methods for Si_3N_4 NSs, which have an index of refraction of about 2, result in very nonuniform diameter NSs. Future improvements in the synthesis of high index of refraction nanospheres may enable further improvements in efficiency for NS coated solar cells.

Fig. 3(a) plots the EQE for both the plain c-Si solar cell and c-Si solar cells with PS NSs on top. This EQE measurement is carried out under monochromatic illumination by a halogen lamp coupled to a monochromator. The ratio between the EQE of PS NS Si solar cells compared with plain Si solar cells is plotted as in Fig. 3(b). There is an EQE enhancement in most of the spectrum measured. Furthermore, there are several distinct peaks for the PS NS coated solar cell EQE. Most notably, at the wavelengths of 470 nm and 1003 nm, the EQE enhancement is almost double that of the plain c-Si solar cell.

In order to better understand the results, we performed finite difference time domain (FDTD) simulations to investigate the absorption in c-Si layer. The simulated structure was like the experimental structure and consisted of 15 μm c-Si with a 200 nm layer of ITO on the front. The back contact was modeled as a perfect electric conductor boundary condition and appropriate symmetric and anti-symmetric boundary conditions are used to model the periodic nature of the NS array. The optical constants of ITO used in the simulation were acquired via ellipsometery from a sputtered ITO film and shown in the Supporting Information. The optical constants of PS [21] and the refractive index of c-Si [22] were both obtained from the literature. In the simulations, we obtained the absorption in

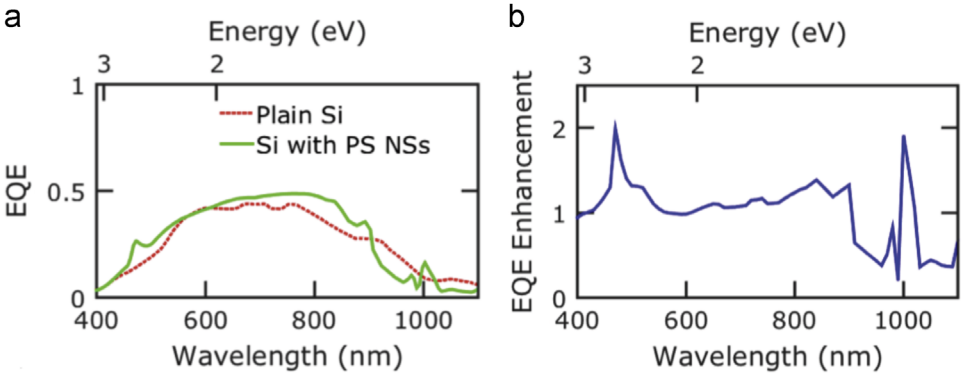

Fig. 3 (a) EQE measured on flat silicon solar cells without and with PS NSs coating. (b) Ratio between EQE of plain Si and Si with PS NSs solar cells versus wavelength.

the c-Si layers for both the plain c-Si and Si with PS NSs solar cells by integrating the position dependent absorption per unit volume over the Si volume. This omits the parasitic absorption that occurs in the ITO thin film, which is also plotted in the Supporting Information. The addition of the PS NSs only changes the parasitic absorption in the ITO thin film negligibly. Fig. 4 plots the absorption of the c-Si from the simulation. Similar to the our experimental EQE results, we find that the absorption in the c-Si layer with PS NSs is higher than that of the plain Si over a broad wavelength range. Furthermore, there are several extra peaks in the absorption spectrum for the structure with PS array.

To understand the extra peaks in EQE and absorption for the structure with PS monolayer, we then investigated the electric field profile at these specific wavelengths for both structures. Fig. 5 plots the electric field intensity $|\mathbf{E}|^2$ at the wavelengths (a) 481 and (b) 756 nm. The c-Si absorption of the plain Si solar cell is 0.57 and 0.46 at these wavelengths, respectively. In contrast, the c-Si absorption of the Si with PS NSs solar cell is 0.78 and 0.57 at these wavelengths, respectively. In Fig. 5, parts (i) and (ii) plot the electric field intensity for the plain Si solar cell, while parts (iii) and (iv) plot the electric field intensity for the solar cell with PS NSs. Parts (i) and (iii) plot the electric field intensity in the x-y plane at $z = -500$ nm. This is 500 nm below the top surface of the Si. Part (ii) and (iv) plot the electric field intensity in the x-z plane at $x=0$. The edges of the nanospheres are shown with white solid lines and the edges of ITO are indicated by white dashed lines. The ultrathin c-Si is underneath the ITO layer and only the top 1000 nm is shown. From part (iii), we can observe the modes of NSs couple to each other because the spheres are touching. These resonant modes exhibit high field intensity in the NSs and allow incident light to couple into the underlying Si across a broader range of wavelengths.

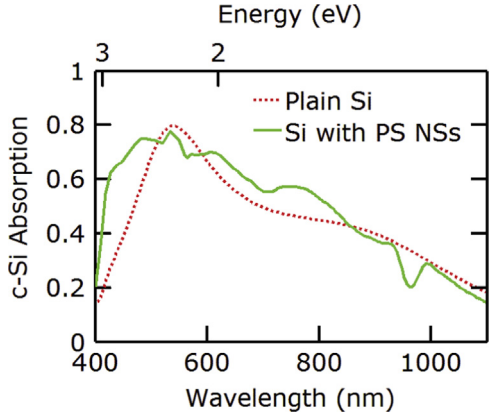

Fig. 4 Simulated absorption spectra in c-Si thin film without and with PS nanospheres coating.

Conclusions

In conclusion, we demonstrate that with a monolayer of 800 nm diameter PS NSs, the light absorption can be enhanced over a broad wavelength range for 15 μm thickness ultrathin c-Si solar cells both in experiments and simulations. This light harvesting scheme results in a 26.5% PCE enhancement and an EQE enhancement of almost 2 times at several wavelengths. The NS array couples incident light into the underlying Si and facilitates wave propagation in the lateral direction. The fabrication technique for this reported light harvesting structure is facile and easy to integrate with other light trapping and anti-reflection techniques. This light harvesting mechanism should be a promising path toward high efficiency and low

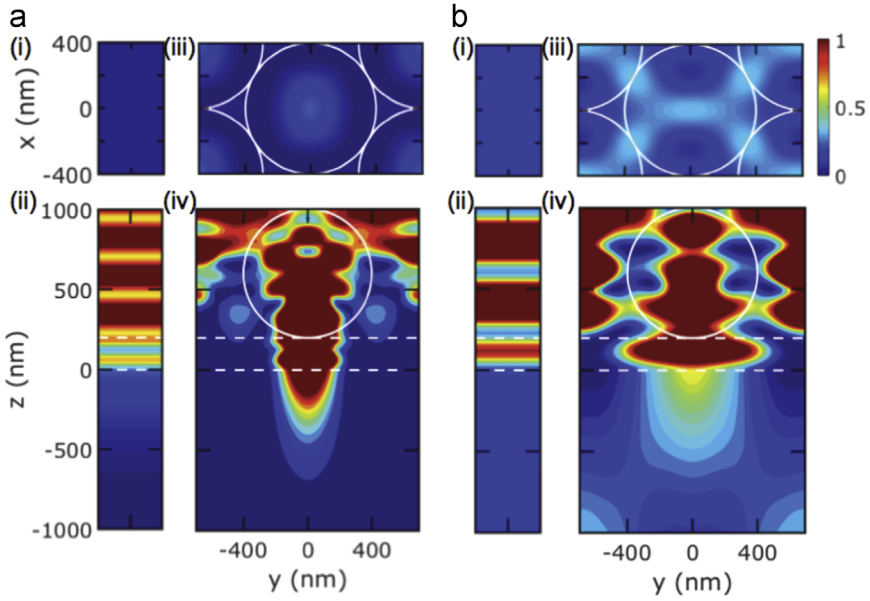

Fig. 5 The electric field intensity $|\mathbf{E}|^2$ at λ=(a) 481 and (b) 756 nm. At each wavelength, the electric field intensity for the (i, ii) plain Si and (iii, iv) Si with PS NS solar cell structures are plotted. Dashed lines show the boundary of the ITO and white lines show the boundaries of the PS NSs. The plain Si solar cell is plotted in (i) the x-y plane at $z = -500$ nm and (ii) the x-z plane cross section view. The Si solar cell with NSs is plotted in (iii) the x-y plane at $z = -500$ nm and (iv) the x-z plane cross section view at $x=0$.

cost solar cells and may be beneficial to other optoelectronic devices.

Acknowledgments

This work was supported by the NSF award CMMI 1233151.

Appendix A. Supplementary data

Supplementary data associated with this paper can be found in the online version at http://dx.doi.org/10.1016/j.nanoen.2015.10.039.

References

[1] A. Blakers, T. Armour, Sol. Energy Mater. Sol. Cell 93 (2009) 1440–1443.
[2] J. Yoon, A.J. Baca, S.-I. Park, P. Elvikis, J.B. Geddes, L. Li, R. H. Kim, J. Xiao, S. Wang, T.-H. Kim, M.J. Motala, B.Y. Ahn, E. B. Duoss, J.A. Lewis, R.G. Nuzzo, P.M. Ferreira, Y. Huang, A. Rockett, J.A. Rogers, Nat. Mater. 7 (2008) 907–915.
[3] S. Wang, B.D. Weil, Y. Li, K.X. Wang, E. Garnett, S. Fan, Y. Cui, Nano Lett. 13 (2013) 4393–4398.
[4] B. Wang, P.W. Leu, Nano Energy 13 (2015) 226–232.
[5] V. Sivakov, G. Andr, A. Gawlik, A. Berger, J. Plentz, F. Falk, S. H. Christiansen, Nano Lett. 9 (2009) 1549–1554 PMID: 19281253.
[6] L. Tsakalakos, J. Balch, J. Fronheiser, B.A. Korevaar, O. Sulima, J. Rand, Appl. Phys. Lett. 91 (2007) 233117.
[7] D.R. Abujetas, R. Paniagua-Domnguez, J. Snchez-Gil, ACS Photon. 2 (2015) 921–929.
[8] A. Shang, X. Zhai, C. Zhang, Y. Zhan, S. Wu, X. Li, Prog. Photovolt.: Res. Appl. (2015), http://dx.doi.org/10.1002/pip.2613.
[9] B. Hua, B. Wang, M. Yu, P.W. Leu, Z. Fan, Nano Energy 5 (2013). http://dx.doi.org/10.1016/j.nanoen.2013.03.016.
[10] K. Peng, X. Wang, L. Li, X. Wu, S. Lee, J. Am. Chem. Soc. 132 (2010) 6872–6873.
[11] Z.Y. Wang, R.J. Zhang, S.Y. Wang, M. Lu, X. Chen, Y.X. Zheng, L.Y. Chen, Z. Ye, C.Z. Wang, K.M. Ho, Sci. Rep. 5 (2015).
[12] B. Wang, P.W. Leu, Nanotechnology 23 (2012) 194003.
[13] C. Hsu, S.T. Connor, M.X. Tang, Y. Cui, Appl. Phys. Lett. 93 (2008) 133109.
[14] T. Gao, E. Stevens, J. kun Lee, P.W. Leu, Opt. Lett. 39 (2014) 4647–4650.
[15] L.-B. Luo, C. Xie, X.-H. Wang, Y.-Q. Yu, C.-Y. Wu, H. Hu, K.-Y. Zhou, X.-W. Zhang, J.-S. Jie, Nano Energy 9 (2014) 112–120.
[16] V.E. Ferry, L.A. Sweatlock, D. Pacifici, H.A. Atwater, Nano Lett. 8 (2008) 4391–4397.
[17] G.D. Moon, T.I. Lee, B. Kim, G. Chae, J. Kim, S. Kim, J.-M. Myoung, U. Jeong, ACS Nano 5 (2011) 8600–8612.
[18] J.C. Hulteen, J. Vac. Sci. Technol. A 13 (1995) 1553.
[19] C.L. Haynes, R.P. Van Duyne, J. Phys. Chem. B 105 (2001) 5599–5611.
[20] G.-J. Lin, H.-P. Wang, D.-H. Lien, P.-H. Fu, H.-C. Chang, C.-H. Ho, C.-A. Lin, K.-Y. Lai, J.-H. He, Nano Energy 6 (2014) 36–43.
[21] X. Ma, J.Q. Lu, R.S. Brock, K.M. Jacobs, P. Yang, X.-H. Hu, Phys. Med. Biol. 48 (2003) 4165.
[22] E.D. Palik, Handbook of Optical Constants of Solids, Academic Press, San Diego, 1997.
[23] J.M. Ball, S.D. Stranks, M.T. Horantner, S. Huttner, W. Zhang, E.J.W. Crossland, I. Ramirez, M. Riede, M.B. Johnston, R. H. Friend, H.J. Snaith, Energy Environ. Sci. 8 (2015) 602–609.

Baomin Wang received his Bachelor of Eng. from the department of Materials Science and Engineering, Tsinghua University, China, in 2010. He is currently pursuing his Ph.D. degree under Dr. Leu at the University of Pittsburgh, USA. His research focuses on simulation and experimental fabrication of nanostructured optoelectronics and plasmonics.

Tongchuan Gao received his Bachelor of Eng. from the department of Materials Science and Engineering, Tsinghua University, China, in 2011. He is currently pursuing his Ph.D. degree under Dr. Leu at the University of Pittsburgh, USA. His research focuses on simulation and experimental fabrication of transparent conductor and plasmonics.

Dr. Paul W. Leu received his B.S. in Mechanical Engineering from Rice University in 2002. He received his M.S. and Ph.D. from Stanford University in 2006 and 2008 respectively. From 2008-10, he worked as a postdoctoral fellow in the department of Electrical Engineering and Computer Sciences at the University of California, Berkeley with a joint appointment at Lawrence Berkeley National Laboratory. He has been an Assistant Professor in the Department of Industrial Engineering at the University of Pittsburgh since August, 2010. His research group's areas of expertise include solar cells, nanomanufacturing, and simulation-based design.